Title

Intravoxel incoherent motion (IVIM) modeling of diffusion MRI during chemoradiation predicts therapeutic response in IDH wildtype glioblastoma

Authors

Maralani, Pejman Jabehdar
Myrehaug, Sten
Mehrabian, Hatef
et al.

Publication Date

2021-03-01

DOI

10.1016/j.radonc.2020.12.037

Peer reviewed

HHS Public Access

Author manuscript

Radiother Oncol. Author manuscript; available in PMC 2021 June 08.

Published in final edited form as:

Radiother Oncol. 2021 March ; 156: 258–265. doi:10.1016/j.radonc.2020.12.037.

Intravoxel incoherent motion (IVIM) modeling of diffusion MRI during chemoradiation predicts therapeutic response in IDH wildtype glioblastoma

Pejman Jabehdar Maralani[a,*], **Sten Myrehaug**[b], **Hatef Mehrabian**[b], **Aimee K.M. Chan**[a], **Max Wintermark**[c], **Chris Heyn**[a], **John Conklin**[d], **Benjamin M. Ellingson**[e], **Saba Rahimi**[f], **Angus Z Lau**[g], **Chia-Lin Tseng**[b], **Hany Soliman**[b], **Jay Detsky**[b], **Shadi Daghighi**[a], **Julia Keith**[h], **David G. Munoz**[h], **Sunit Das**[i], **Eshetu G. Atenafu**[j,1], **Nir Lipsman**[i], **James Perry**[k], **Greg Stanisz**[g], **Arjun Sahgal**[b]

[a]Department of Medical Imaging, Sunnybrook Health Sciences Center, University of Toronto, Canada;

[b]Department of Radiation Oncology, Sunnybrook Health Sciences Center, University of Toronto, Canada;

[c]Department of Radiology, Stanford University, United States;

[d]Department of Radiology, Massachusetts General Hospital, United States;

[e]Department of Radiological Sciences and Psychiatry, University of California Los Angeles, United States;

[f]Department of Biomedical Engineering, University of Toronto, Canada;

[g]Department of Medical Biophysics, Sunnybrook Research Institute, University of Toronto, Canada;

[h]Department of Laboratory Medicine and Pathobiology, University of Toronto, Canada;

[i]Department of Surgery, Division of Neurosurgery, University of Toronto, Canada;

[j]Department of Biostatistics, University Health Network, Canada;

[k]Department of Medicine, Division of Neurology, University of Toronto, Canada;

Abstract

Background: Prediction of early progression in glioblastoma may provide an opportunity to personalize treatment. Simplified intravoxel incoherent motion (IVIM) MRI offers quantitative

[*]Corresponding author at: AG270C-2075 Bayview Avenue, Toronto, Ontario, Canada. Pejman.Maralani@sunnybrook.ca (P. Jabehdar Maralani), e.atenafu@utoronto.ca (E.G. Atenafu).

[1]Responsible for statistical analyses.

Declaration of Competing Interest

The authors declare that they have no known competing financial interests or personal relationships that could have appeared to influence the work reported in this paper.

Appendix A. Supplementary data

Supplementary data to this article can be found online at https://doi.org/10.1016/j.radonc.2020.12.037.

estimates of diffusion and perfusion metrics. We investigated whether these metrics, during chemoradiation, could predict treatment outcome.

Methods: 38 patients with newly diagnosed IDH-wildtype glioblastoma undergoing 6-week/30-fraction chemoradiation had standardized post-operative MRIs at baseline (radiation planning), and at the 10th and 20th fractions. Non-overlapping T1-enhancing (T1C) and non-enhancing T2-FLAIR hyperintense regions were independently segmented. Apparent diffusion coefficient (ADC_{T1C}, $ADC_{T2\text{-}FLAIR}$) and perfusion fraction (f_{T1C}, $f_{T2\text{-}FLAIR}$) maps were generated with simplified IVIM modelling. Parameters associated with progression before or after 6.9 months (early vs late progression, respectively), overall survival (OS) and progression-free survival (PFS) were investigated.

Results: Higher $ADC_{T2\text{-}FLAIR}$ at baseline [Odds Ratio (OR) = 1.06, 95% CI 1.01–1.15, p = 0.025], lower $f_{T2\text{-}FLAIR}$ at fraction 10 (OR = 2.11, 95% CI 1.04–4.27, p = 0.018), and lack of increase in $ADC_{T2\text{-}FLAIR}$ at fraction 20 compared to baseline (OR = 1.12, 95% CI 1.02–1.22, p = 0.02) were associated with early progression. Combining $ADC_{T2\text{-}FLAIR}$ at baseline, $f_{T2\text{-}FLAIR}$ at fraction 10, ECOG and MGMT promoter methylation status significantly improved AUC to 90.3% compared to a model with only ECOG and MGMT promoter methylation status (p = 0.001). Using multivariable analysis, neither IVIM metrics were associated with OS but higher $f_{T2\text{-}FLAIR}$ at fraction 10 (HR = 0.72, 95% CI 0.56–0.95, p = 0.018) was associated with longer PFS.

Conclusion: $ADC_{T2\text{-}FLAIR}$ at baseline, its lack of increase from baseline to fraction 20, or $f_{T2\text{-}FLAIR}$ at fraction 10 significantly predicted early progression. $f_{T2\text{-}FLAIR}$ at fraction 10 was associated with PFS.

Keywords

Glioblastoma; Survival; Progression-free Survival; Diffusion MRI; Intravoxel incoherent motion imaging; Radiotherapy

---

For patients with glioblastoma, median survival has not significantly changed from 6.9 months since the landmark Stupp trial in 2005 [1]. The current standard of care is maximal safe surgical resection followed by chemoradiation. The radiation planning MRI is the last imaging timepoint before the start of chemoradiation. Subsequently, the first MRI is obtained 6–8 weeks after completing chemoradiation, translating to approximately 3 months where no imaging is performed.

The challenge with early imaging response determination is threefold. First, we do not routinely image during chemoradiation; therefore, there is no information beyond clinical assessments until the first post-chemoradiation MRI. Second, the interpretation of the first post-chemoradiation MRI is confounded by changes associated with radiation, such as pseudoprogression [2,3]. Lastly, we remain reliant on crude changes in 2-dimensional measurements from standard MRI to determine response without advanced quantitative imaging. Should we have the ability to know during or soon after chemoradiation which patients would not benefit from standard of care using imaging biomarkers, we could better individualize patient care pathways early on.

Intravoxel incoherent motion (IVIM) imaging is based on diffusion-weighted imaging (DWI) MRI and can provide separate estimates for quantitative metrics of diffusion, representative of structural changes [4], and the perfusion fraction [5] which is a measure related to microcirculation. Furthermore, it has the benefit of not requiring the use of gadolinium-based contrast agents, and short acquisition times. Few studies have investigated diffusion and/or perfusion MRI parameters in glioblastoma during chemoradiation [6–8], and they have been limited with respect to: sample size; assessment of only enhancing tumor as opposed to non-enhancing T2-FLAIR hyperintense regions; mixed sample populations including patients with recurrent glioblastoma on Bevacizumab or other clinical trial drugs; and/or, typically the intra-treatment MRI was acquired at only one timepoint over the course of chemoradiation. A summary of these differences is provided in Supplementary Table 1 [6–18].

We propose using a previously validated simplified IVIM model [19,20] to investigate the prognostic potential of diffusion and perfusion metrics at multiple timepoints over the course of chemoradiation in patients with glioblastoma, with the enhancing tumor and surrounding non-enhancing T2-FLAIR hyperintense regions interrogated separately. For the simplified IVIM model, 3 b-values were be used (0, 500, and 1000 s/mm^2), as this follows consensus guidelines for brain tumor imaging in clinical trials for DWI [21] and confers the additional benefit of not requiring specialized hardware or pulse sequence design.

Materials & methods

Patient population

This prospective study was approved by the local institutional Research Ethics Board (#430–2015). Written informed consent was obtained from all patients. A total of 50 consecutive patients with a potential new high-grade glioma diagnosis on neuroimaging were considered for recruitment. Twelve patients were excluded: four with WHO grade II or III gliomas on pathology; three withdrew; three discontinued chemoradiation; one progressed with treatment interruptions; and one had an IDH mutation, which is a distinctly different molecular and clinical profile compared to IDH wildtype (IDHwt) glioblastoma [22]. Therefore, a total of 38 patients with IDHwt glioblastoma who completed standard radiation (60 Gy in 30 fractions) concurrent with temozolomide were included. Prognostic factors such as age at diagnosis, Eastern Cooperative Oncology Group (ECOG) performance status, extent of resection, IDH status and MGMT promoter methylation status ($MGMT_{PMS}$) were extracted from electronic medical records.

MR imaging

All patients were scanned on a single 1.5 T Philips Ingenia system (Philips Medical Systems, Best, The Netherlands). Acquired sequences included 3D T2-FLAIR, pre- and post-contrast 3D T1-weighted (T1) and echo planar DWI with three b-values (0, 500, and 1000 s/mm^2) [21]. DWI was trace-weighted with an average of 3 orthogonal directions, and the addition of the 500 s/mm^2 b-value requires less than a minute of additional scan time compared to scanning with only b-values of 0 and 1000 s/mm^2. No signal averaging was

performed at b = 0 s/mm^2. Detailed imaging parameters are provided in Supplementary Table 2. Patients were scanned at radiation planning, and at fractions 10 and 20.

T2-FLAIR images were coregistered to T1 post-contrast (T1C) images using Elastix registration software [23]. Volumes of interest (VOIs) were then manually delineated using the semi-automatic thresholding software Amira (version 2019.2, Thermo Fischer Scientific, Berlin, Germany). VOIs consisted of non-overlapping T1 enhancing (Fig. 1A, 1F) and surrounding nonenhancing T2-FLAIR hyperintense regions (Fig. 1B, 1G). Areas of intrinsic T1 hyperintensity representing hemorrhagic material were not included in T1C contour delineations. Necrotic/cystic regions, surgical cavity and large vessels were excluded from all VOIs. VOIs were then coregistered to b = 0 of DWI and re-sampled with the resolution of the DWI sequence (Fig. 1C–E). VOIs were also drawn on the contralateral normal appearing white matter (cNAWM) and grey matter (cNAGM). No eddy current correction was performed.

MRI quantification

A previously validated simplified IVIM model [19,20] was used to calculate the diffusion coefficient (D, Fig. 1D) and perfusion fraction (f, Fig. 1E) maps. The technique assumes the DWI signal loss due to blood flow in the microvasculature has negligible contribution to DWI images acquired at high b-values. As in prior studies [19,24], voxels with values of $f <$ 0% or $f >$ 30% were considered non-physiological and excluded.

In order to provide a diffusion metric that is widely used clinically and to enable comparison with literature, the apparent diffusion coefficient (ADC) was also calculated using the slope of the natural logarithm of the b = 1000 over b = 0 images (Fig. 1C).

Statistics

Parametric maps were calculated voxelwise, and expressed as median and interquartile range (IQR) over the VOIs. All outcome definitions were calculated using the date of the baseline (post-surgical radiation planning) MRI as reference.

The primary endpoint of the study was to determine whether IVIM metrics could be used to predict progression before or after 6.9 months (209 days), the median time to progression reported by Stupp et al. [1]. The secondary endpoint of the study was to see if the same metrics were associated with progression-free survival (PFS) and overall survival (OS). PFS was defined as the time until disease progression in accordance with RANO criteria [25], and the date of death or last follow-up was used to calculate OS, both in months. PFS and OS were calculated using the Kaplan-Meier product-limit method and differences were assessed using the log-rank test. Cox regression was used for multivariable survival analyses.

Significant findings on univariate analyses were tested in multivariable analyses. Logistic regression analysis was used to assess the association of ADC, D, and f with early vs. late progression, and the performance was assessed using the area under the receiver operating characteristic curve (AUC). All p-values were two-sided, and a $p < 0.05$ was considered

statistically significant. Statistical analysis was performed using SAS (version 9.4 for Windows; SAS Institute, Inc., Cary, NC, USA).

Results

Patient details are summarized in Table 1. Age at diagnosis ($p = 0.74$), extent of resection ($p = 0.68$), $MGMT_{PMS}$ ($p = 0.18$) and ECOG ($p = 0.06$) were not significantly associated with early or late progression in univariate analyses. Due to limited sample size, we assessed the impact of the age [26], extent of resection [27], $MGMT_{PMS}$ [28], and ECOG [29] on PFS and OS via univariate analyses to determine what covariates should be included in multivariable analyses; only $MGMT_{PMS}$ and ECOG were significant (Supplementary Fig. 1) and included in further analyses.

Five patients (13%) demonstrated pseudoprogression within the follow-up period. With retrospective follow-up, all five cases were confirmed to have true progression after 6.9 months, and therefore were considered late progressors.

Median ADC_{cNAWM} was 0.76×10^{-3} mm^2/s (IQR, 0.72–0.78 $\times 10^{-3}$ mm^2/s) and median ADC_{cNAGM} was 0.88×10^{-3} mm^2/s (IQR, 0.82–0.92 $\times 10^{-3}$ mm^2/s). Median ADC values stratified by the timepoint of acquisition, VOI, and progression status are summarized in Table 2 and Fig. 2A–B. Higher $ADC_{T2\text{-}FLAIR}$ at baseline was significantly associated with early progression after adjusting for ECOG and $MGMT_{PMS}$ (adjusted OR (aOR) = 1.06, 95% CI 1.00–1.01, $p = 0.025$). Using the median as the cut-off (1.07×10^{-3} mm^2/s) within $ADC_{T2\text{-}FLAIR}$ to predict early vs late progression, yielded a sensitivity and specificity of 76.5% and 66.7%, respectively. No significant associations with early progression were observed at any other timepoint for ADC_{T1C} nor $ADC_{T2\text{-}FLAIR}$.

When assessing changes in the ADC relative to baseline, ADC_{T1C} continually increased although these changes were not significantly associated with outcome (fraction 10, $p = 0.17$; fraction 20, $p = 0.22$). Comparatively, $ADC_{T2\text{-}FLAIR}$ of early progressors did not increase from baseline to fraction 20 whereas ADC of late progressors increased between these timepoints. Lack of increase in $ADC_{T2\text{-}FLAIR}$ from baseline to fraction 20 was associated with early progression (aOR = 1.12, 95% CI 1.02–1.22, $p = 0.02$).

With regards to D, as D is known to approximate ADC when the effect of perfusion fractions are small as in the case for brain [30], their correlation was assessed for every timepoint of acquisition and VOI. At every timepoint and VOI, a correlation above 94.5% and $p < 0.0001$ were observed. To prevent multicollinearity, and since ADC is more commonly used in the clinical setting, all subsequent analyses was performed using ADC rather than D. Further details on D are provided in the Supplementary Table 3 and Supplementary Fig. 2.

With regards to f, median f_{cNAWM} was 10.4% (IQR, 9.7–11.6%) and median f_{cNAGM} was 12.5% (IQR, 11.1–12.9%). Median f, stratified by timepoint of acquisition, VOI, and progression status are shown in Table 2 and Fig. 2C–D. Early progressors demonstrated lower f at all timepoints, although this was only significant at fraction 10 where lower f was associated with early progression in both T1C (aOR = 1.87, 95% CI 1.11–3.15, $p = 0.018$) and T2-FLAIR (aOR = 2.11, 95% CI 1.04–4.27, $p = 0.039$). Using the median as the cut-off

(12%) for $f_{T2\text{-}FLAIR}$ at fraction 10 to predict early vs late progression, yielded a sensitivity and specificity of 70.6% and 66.7%, respectively. Similarly, using the median as the cut-off (15%) for f_{T1C} at fraction 10 yielded a sensitivity and specificity of 64.7% and 61.9%, respectively.

When assessing changes in f relative to baseline, no significant changes for f_{T1C} (fraction 10, $p = 0.30$; fraction 20, $p = 0.24$) or $f_{T2\text{-}FLAIR}$ (fraction 10, $p = 0.75$; fraction 20, $p = 0.98$) were observed, and none were associated with early progression.

When assessing our primary endpoint, median $ADC_{T2\text{-}FLAIR}$ at baseline, f_{T1C} and $f_{T2\text{-}FLAIR}$ at fraction 10 were combined into a single model and adjusted for ECOG and $MGMT_{PMS}$ to assess whether these variables could better predict progression status (early vs late). f_{T1C} at fraction 10 was not significant in the presence of median of $ADC_{T2\text{-}FLAIR}$ at baseline and $f_{T2\text{-}FLAIR}$ at fraction 10 ($p = 0.15$), and therefore was not included in subsequent multivariable analyses.

To assess the contribution of $ADC_{T2\text{-}FLAIR}$ and $f_{T2\text{-}FLAIR}$ in predicting outcome, we compared the performance between the combinations of ECOG and $MGMT_{PMS}$ *vs* $ADC_{T2\text{-}FLAIR}$ and $f_{T2\text{-}FLAIR}$ *vs* all 4 parameters together. The model with ECOG and $MGMT_{PMS}$ had an AUC of 73.4%, whereas IVIM parameters had an AUC of 83.9%. The combination of all 4 parameters in a model was significantly improved with an AUC of 90.3% ($p = 0.001$). In the multivariable model, all parameters except for ECOG (aOR = 0.15, 95% CI 0.02–1.14, $p = 0.066$) were significant ($ADC_{T2\text{-}FLAIR}$, aOR = 1.08, 95% CI 1.01–1.15, $p = 0.028$; $f_{T2\text{-}FLAIR}$, aOR = 2.32, 95% CI 1.07–5.05, $p = 0.034$; $MGMT_{PMS}$, aOR = 0.08, 95% CI 0.01–0.86, $p = 0.039$).

When assessing our secondary endpoint using Kaplan Meier, the median $ADC_{T2\text{-}FLAIR}$ at baseline (1.07×10^{-3} mm^2/s) was significantly associated with OS ($p = 0.037$; Fig. 3A) but not PFS ($p = 0.48$; Fig. 3C), with higher $ADC_{T2\text{-}FLAIR}$ significantly associated with a shorter OS. Conversely, the median $f_{T2\text{-}FLAIR}$ at fraction 10 (12%) was significantly associated with PFS ($p = 0.016$; Fig. 3D) but not OS ($p = 0.48$, Fig. 3B), with lower $f_{T2\text{-}FLAIR}$ significantly associated with shorter PFS. Combining these parameters, patients with both high $ADC_{T2\text{-}FLAIR}$ and low $f_{T2\text{-}FLAIR}$ had significantly worse OS ($p = 0.026$) and PFS ($p = 0.002$).

Results from Cox regression are summarized in Table 3. While an ECOG of 0 and methylated $MGMT_{PMS}$ demonstrated significant associations with longer OS (HR = 0.19, 95% CI 0.063–0.59, $p = 0.004$; and HR = 0.28, 95% CI 0.1–0.8, $p = 0.017$, respectively), neither IVIM parameters were significant. Higher $f_{T2\text{-}FLAIR}$ (HR = 0.72, 95% CI 0.56–0.95, $p = 0.018$) and methylated $MGMT_{PMS}$ (HR = 0.25, 95% 0.1–0.63, $p = 0.003$) were associated with longer PFS.

Discussion

ADC and f of the entire T1C, and the surrounding nonenhancing T2-FLAIR volumes, were evaluated before and during chemoradiation in patients with newly diagnosed, IDHwt glioblastoma. While there are advantages to more sophisticated IVIM models (e.g., ability to

calculate the pseudo-diffusion coefficient, D^* [12]), we chose the simplified model to increase the generalizability and clinical utility of the results. We demonstrated that various quantitative metrics from the T2-FLAIR at baseline, and at fractions 10 and 20, can act as prognostic biomarkers. Metrics from the T2-FLAIR volume exhibited stronger associations with outcome compared to those from the T1C volume, with $f_{\text{T2-FLAIR}}$ significantly predictive of PFS.

We report that the use of the simplified IVIM model here generated similar values for ADC within the cNAWM and cNAGM as those reported in the literature [31–33], and similarly for f_{cNAWM} [12,14,19,24,34–36] and f_{cNAGM} [36,43], lending strength to our results.

We further report that at baseline, a greater $\text{ADC}_{\text{T2-FLAIR}}$ value is significantly associated early progression, and trended towards worse OS. While previous, single time-point studies found that lower ADC was associated with poorer outcomes [9,12] (Supplementary Table 1), significant methodological differences may be the cause of this discordance. In these earlier studies, circular regions of interest were drawn over areas of highest and lowest ADC on the pre-operative MRI of patients with grade 2 to 4 gliomas. Comparatively, we reported on the entirety of the T1C and T2-FLAIR regions on post-operative MRI, where all or most of the enhancing tumor has already been resected, as most (81.6%) of our cases underwent gross- or sub- total resection. In addition, on radiation planning MRI the T1C may include tumor but also subacute ischemic changes and granulation tissue compared to the pre-operative MRI where the T1C is only tumor. Moreover, our patient dataset was limited but homogenous, comprising of only patients with wildtype IDH glioblastomas. We hypothesize that greater $\text{ADC}_{\text{T2-FLAIR}}$ after post-surgical resection reflects a more biologically aggressive tumor, which is the cause of earlier progression ($p = 0.029$, Fig. 2B). This effect was also observed in Li et al. [6], who reported higher normalized ADC values in the T2-FLAIR of patients that died within the year compared to those that survived longer, although it was not significantly related to OS or PFS. We surmise that more aggressive tumors cause more disruption of blood brain barrier and increased interstitial edema leading to increased ADC, whereas less aggressive tumors cause less disruption of blood brain barrier.

During chemoradiation, the relative change in the ADC may be more reflective of a direct relationship between cellularity, tumor cell kill, and interstitial edema. We hypothesize that the lack of increase in $\text{ADC}_{\text{T2-FLAIR}}$ by fraction 20 compared to baseline ($p = 0.02$) of early progressors reflects persistent tumour burden or even cell proliferation and hence, represents a surrogate of treatment resistance. This hypothesis is supported by a recent study that utilized functional diffusion maps in patients with Grade 3 and 4 gliomas before and midway through radiotherapy, and found that patients with a high percentage of unchanging ADC compared to baseline had worse prognosis [8]. Similar results were also observed in another study evaluating ADC in patients with brain metastases during a course of 30 Gy in 10 fractions of whole brain radiation therapy, where it was reported that ADC decreased during treatment in non-responding tumors [37], and likewise in Li et al. [6] and Wen et al. [7], who studied post-operative patients with newly diagnosed glioblastoma. However, differences in methodology and the inclusion of patients undergoing mixed therapies limit direct comparison with our results, and none of the studies reported the status of IDH mutation or MGMT_{PMS}.

With regards to *f*, our reported values fall within the large range of values reported in the literature [12,14,19,34,35,38]. This variation is likely due to differences in acquisition protocols and patient populations. We observed *f* to be higher at all timepoints in late progressors within both T2-FLAIR and T1C volumes (Fig. 2C–D). *f* is related to relative cerebral blood volume (rCBV) [5,12] which is highly associated with relative cerebral blood flow (rCBF) in brain tumors [10,39]. Within this context, higher rCBF has been shown to be associated with better prognosis in glioblastoma [40–42]. Therefore, our results are consistent with better overall perfusion within the tumor capillaries and subsequently, better responsiveness during chemoradiation. Furthermore, our results may signify the importance of early vascular normalization processes that enhance perfusion. However, it is also possible that the increase observed is due to a free water effect due to increased interstitial water and edema. Moreover, *f* may be affected by permeability effects, particularly when there is a compromised blood brain barrier. Further studies are required to validate this hypothesis.

To the authors' knowledge, there are a limited number of studies that have investigated *f* in patients with glioblastoma. Puig et al. [10] investigated the association of IVIM metrics with outcomes in patients with newly diagnosed glioblastoma prior to surgery and found that patients with higher f_{T1C} had shorter OS, with no association between $f_{T2\text{-}FLAIR}$ and outcome. Federau et al. [9] also observed a higher *f* within high-grade gliomas, however, no association was observed between the f_{T1C} and OS, and T2-FLAIR was not investigated. Both studies utilized pre-operative MRIs and *f* was calculated using the full IVIM model; VOIs were then manually placed over the highest *f* for analyses. These methodological differences may be the cause of the discrepancies of our results.

When analyzing the combined effect of the median $ADC_{T2\text{-}FLAIR}$ at baseline and median $f_{T2\text{-}FLAIR}$ at fraction 10, adjusted for $MGMT_{PMS}$ and ECOG, $ADC_{T2\text{-}FLAIR}$ trended towards significance for OS whereas $f_{T2\text{-}FLAIR}$ maintained its significance for PFS (Table 3). As $ADC_{T2\text{-}FLAIR}$ was significant on univariate analysis ($p = 0.04$), and a significant increase in AUC was observed when ECOG, $MGMT_{PMS}$, and IVIM parameters were combined ($p = 0.001$), we suspect that the loss of significance for $ADC_{T2\text{-}FLAIR}$ is primarily due to power. We hypothesize that understanding both metrics is important to determine tumour responsiveness.

This study has limitations. The data may be biased due to the single-centre nature of the data; furthermore, all scans were from a single vendor. However, these may also represent a strength as the consistency allows for less variability in the acquisitions. Furthermore, inclusion of the entire T2-FLAIR hyperintensity and T1C as opposed to subjective placement of regions of interest of a defined size is a strength, though validation in a larger, multi-institutional cohort with different scanners is still required. Compared to conventional IVIM models, using only 3 b-values of diffusion images without eddy currents correction affects the accuracy of IVIM parameters leading to the potential for increased variation. However, our suggested model improves feasibility and facilitates translation and implementation into daily clinical practice.

In conclusion, when using simplified IVIM metrics to differentiate early versus late progression, $ADC_{T2\text{-}FLAIR}$ at baseline, as well as $f_{T2\text{-}FLAIR}$ and f_{T1C} at fraction 10 were significant, though f_{T1C} at fraction 10 did not maintain its significance in the presence of the other two parameters. A model combining $ADC_{T2\text{-}FLAIR}$ at baseline, $f_{T2\text{-}FLAIR}$ at fraction 10, $MGMT_{PMS}$ and performance status demonstrated higher AUC compared to when variables were assessed separately. Lack of increase in $ADC_{T2\text{-}FLAIR}$ over the course of chemoradiation was associated with early progression, and can potentially act as an imaging biomarker of response to treatment in differentiating progression. In time-dependent analyses, higher $ADC_{T2\text{-}FLAIR}$ at baseline was significantly associated with shorter OS, and a lower $f_{T2\text{-}FLAIR}$ at fraction 10 was associated with shorter PFS. In a multivariable model with ECOG and $MGMT_{PMS}$, no IVIM metrics were significantly associated with OS, however $f_{T2\text{-}FLAIR}$ at fraction 10 retained its significance with PFS.

Supplementary Material

Refer to Web version on PubMed Central for supplementary material.

Abbreviations:

DWI	diffusion-weighted imaging
T2-FLAIR	T2-weighted fluid-level attenuated inversion recovery
IVIM	intravoxel incoherent motion
IDH	isocitrate dehydrogenase 1
IDHwt	wildtype IDH
ECOG	Eastern Cooperative Oncology Group
MGMT	O^6-methylguanine-DNA methyltransferase
VOI	volume of interest
cNAWM	contralateral normal appearing white matter
cNAGM	contralateral normal appearing grey matter
ADC	apparent diffusion coefficient
RANO	response assessment in neuro-oncology
AUC	area under the receiver operating characteristic curve
aOR	adjusted odds ratio

References

[1]. Stupp R, Mason WP, van den Bent MJ, Weller M, Fisher B, Taphoorn MJB, et al. Radiotherapy plus concomitant and adjuvant temozolomide for glioblastoma. N Engl J Med 2005;352(10):987–96. [PubMed: 15758009]

[2]. Taal W, Brandsma D, de Bruin HG, Bromberg JE, Swaak-Kragten AT, Sillevis Smitt PAE, van Es CA, van den Bent MJ. Incidence of early pseudo-progression in a cohort of malignant glioma patients treated with chemoirradiation with temozolomide. Cancer 2008;113(2):405–10. [PubMed: 18484594]

[3]. Hygino da Cruz LC Jr, Rodriguez I, Domingues RC, Gasparetto EL, Sorensen AG. Pseudoprogression and pseudoresponse: imaging challenges in the assessment of posttreatment glioma. AJNR Am J Neuroradiol 2011;32(11):1978–85. [PubMed: 21393407]

[4]. Iima M, Le Bihan D. Clinical intravoxel incoherent motion and diffusion MR imaging: past, present, and future. Radiology 2016;278(1):13–32. [PubMed: 26690990]

[5]. Bihan DL, Turner R. The capillary network: a link between ivim and classical perfusion. Magn. Reson. Med 1992;27(1):171–8. [PubMed: 1435202]

[6]. Li Y, Lupo JM, Polley M-Y, Crane JC, Bian W, Cha S, Chang S, Nelson SJ. Serial analysis of imaging parameters in patients with newly diagnosed glioblastoma multiforme. Neuro-Oncology 2011;13(5):546–57. [PubMed: 21297128]

[7]. Wen Q, Jalilian L, Lupo JM, Molinaro AM, Chang SM, Clarke J, Prados M, Nelson SJ. Comparison of ADC metrics and their association with outcome for patients with newly diagnosed glioblastoma being treated with radiation therapy, temozolomide, erlotinib and bevacizumab. J Neurooncol 2015;121(2):331–9. [PubMed: 25351579]

[8]. Chenevert TL, Malyarenko DI, Galbán CJ, Gomez-Hassan DM, Sundgren PC, Tsien CI, et al. Comparison of voxel-wise and histogram analyses of glioma ADC maps for prediction of early therapeutic change. Tomography. 2019;5:7–14. [PubMed: 30854437]

[9]. Federau C, Cerny M, Roux M, Mosimann PJ, Maeder P, Meuli R, Wintermark M. IVIM perfusion fraction is prognostic for survival in brain glioma. Clin Neuroradiol 2017;27(4):485–92. [PubMed: 27116215]

[10]. Puig J, Sánchez-González J, Blasco G, Daunis IEP, Federau C, Alberich-Bayarri Á, et al. Intravoxel incoherent motion metrics as potential biomarkers for survival in glioblastoma. PLoS One. 2016;11:e0158887. [PubMed: 27387822]

[11]. Barajas RF Jr, Hodgson JG, Chang JS, Vandenberg SR, Yeh R-F, Parsa AT, et al. Glioblastoma multiforme regional genetic and cellular expression patterns: influence on anatomic and physiologic MR imaging. Radiology 2010;254 (2):564–76. [PubMed: 20093527]

[12]. Federau C, Meuli R, O'Brien K, Maeder P, Hagmann P. perfusion measurement in brain gliomas with intravoxel incoherent motion MRI. Am J Neuroradiol 2014;35(2):256–62. [PubMed: 23928134]

[13]. Elson A, Paulson E, Bovi J, Siker M, Schultz C, Laviolette PS. Evaluation of pre-radiotherapy apparent diffusion coefficient (ADC): patterns of recurrence and survival outcomes analysis in patients treated for glioblastoma multiforme. J Neurooncol 2015;123(1):179–88. [PubMed: 25894597]

[14]. Hu YC, Yan LF, Wu L, Du P, Chen BY, Wang L, et al. Intravoxel incoherent motion diffusion-weighted MR imaging of gliomas: efficacy in preoperative grading. Sci Rep. 2014;4:7208. [PubMed: 25434593]

[15]. Moffat BA, Chenevert TL, Lawrence TS, Meyer CR, Johnson TD, Dong Q, Tsien C, Mukherji S, Quint DJ, Gebarski SS, Robertson PL, Junck LR, Rehemtulla A, Ross BD. Functional diffusion map: A noninvasive MRI biomarker for early stratification of clinical brain tumor response. Proc Natl Acad Sci 2005;102 (15):5524–9. [PubMed: 15805192]

[16]. Hamstra DA, Chenevert TL, Moffat BA, Johnson TD, Meyer CR, Mukherji SK, Quint DJ, Gebarski SS, Fan X, Tsien CI, Lawrence TS, Junck L, Rehemtulla A, Ross BD. Evaluation of the functional diffusion map as an early biomarker of time-to-progression and overall survival in high-grade glioma. Proc Natl Acad Sci 2005;102(46):16759–64. [PubMed: 16267128]

[17]. Hamstra DA, Galbán CJ, Meyer CR, Johnson TD, Sundgren PC, Tsien C, Lawrence TS, Junck L, Ross DJ, Rehemtulla A, Ross BD, Chenevert TL. Functional diffusion map as an early imaging biomarker for high-grade glioma: correlation with conventional radiologic response and overall survival. JCO 2008;26(20):3387–94.

[18]. Shen N, Zhao L, Jiang J, Jiang R, Su C, Zhang S, Tang X, Zhu W. Intravoxel incoherent motion diffusion-weighted imaging analysis of diffusion and microperfusion in grading gliomas and

comparison with arterial spin labeling for evaluation of tumor perfusion: IVIM MRI in Grading Gliomas. J. Magn. Reson. Imaging 2016;44(3):620–32. [PubMed: 26880230]

[19]. Conklin J, Heyn C, Roux M, Cerny M, Wintermark M, Federau C. A Simplified model for intravoxel incoherent motion perfusion imaging of the brain. AJNR Am J Neuroradiol 2016;37(12):2251–7. [PubMed: 27561834]

[20]. Le Bihan D, Breton E, Lallemand D, Aubin ML, Vignaud J, Laval-Jeantet M. Separation of diffusion and perfusion in intravoxel incoherent motion MR imaging.. Radiology 1988;168(2):497–505. [PubMed: 3393671]

[21]. Ellingson BM, Bendszus M, Boxerman J, Barboriak D, Erickson BJ, Smits M, et al. Consensus recommendations for a standardized Brain Tumor Imaging Protocol in clinical trials. Neuro-oncology. 2015;17:1188–98. [PubMed: 26250565]

[22]. Noushmehr H, Weisenberger DJ, Diefes K, Phillips HS, Pujara K, Berman BP, et al. Identification of a CpG island methylator phenotype that defines a distinct subgroup of glioma. Cancer Cell 2010;17(5):510–22. [PubMed: 20399149]

[23]. Klein S, Staring M, Murphy K, Viergever MA, Pluim J. elastix: A toolbox for intensity-based medical image registration. IEEE Trans. Med. Imaging 2010;29 (1):196–205. [PubMed: 19923044]

[24]. Federau C, Maeder P, O'Brien K, Browaeys P, Meuli R, Hagmann P. Quantitative measurement of brain perfusion with intravoxel incoherent motion MR imaging. Radiology 2012;265(3):874–81. [PubMed: 23074258]

[25]. Wen PY, Macdonald DR, Reardon DA, Cloughesy TF, Sorensen AG, Galanis E, et al. Updated response assessment criteria for high-grade gliomas: response assessment in neuro-oncology working group. JCO 2010;28(11):1963–72.

[26]. Lamborn KR, Chang SM, Prados MD. Prognostic factors for survival of patients with glioblastoma: recursive partitioning analysis. Neuro-oncology. 2004;6:227–35. [PubMed: 15279715]

[27]. Sanai N, Polley M-Y, McDermott MW, Parsa AT, Berger MS. An extent of resection threshold for newly diagnosed glioblastomas: Clinical article. JNS 2011;115(1):3–8.

[28]. Hegi ME, Diserens A-C, Gorlia T, Hamou M-F, de Tribolet N, Weller M, et al. MGMT gene silencing and benefit from temozolomide in glioblastoma. N Engl J Med 2005;352(10):997–1003. [PubMed: 15758010]

[29]. Helseth R, Helseth E, Johannesen TB, Langberg CW, Lote K, Rønning P, et al. Overall survival, prognostic factors, and repeated surgery in a consecutive series of 516 patients with glioblastoma multiforme. Acta Neurol Scand. 2010;122:159–67. [PubMed: 20298491]

[30]. Le Bihan D What can we see with IVIM MRI?. NeuroImage 2019;187:56–67. [PubMed: 29277647]

[31]. Helenius J, Soinne L, Perkiö J, Salonen O, Kangasmäki A, Kaste M, et al. Diffusion-weighted MR imaging in normal human brains in various age groups. AJNR Am J Neuroradiol 2002;23:194–9. [PubMed: 11847041]

[32]. Engelter ST, Provenzale JM, Petrella JR, DeLong DM, MacFall JR. The effect of aging on the apparent diffusion coefficient of normal-appearing white matter. Am J Roentgenol 2000;175(2):425–30. [PubMed: 10915688]

[33]. Qin L, Li A, Qu J, Reinshagen K, Li X, Cheng S-C, Bryant A, Young GS. Normalization of ADC does not improve correlation with overall survival in patients with high-grade glioma (HGG). J Neurooncol 2018;137(2):313–9. [PubMed: 29383647]

[34]. Bisdas S, Koh TS, Roder C, Braun C, Schittenhelm J, Ernemann U, Klose U. Intravoxel incoherent motion diffusion-weighted MR imaging of gliomas: feasibility of the method and initial results. Neuroradiology 2013;55(10):1189–96. [PubMed: 23852430]

[35]. Lin Y, Li J, Zhang Z, Xu Q, Zhou Z, Zhang Z, Zhang Y, Zhang Z. Comparison of intravoxel incoherent motion diffusion-weighted MR imaging and arterial spin labeling MR imaging in gliomas. Biomed Res Int 2015;2015:1–10.

[36]. Wirestam R, Borg M, Brockstedt S, Lindgren A, Holtås S, Ståhlberg F. Perfusion-related parameters in intravoxel incoherent motion MR imaging compared with CBV and CBF measured

by dynamic susceptibility-contrast MR technique. Acta Radiol 2001;42(2):123–8. [PubMed: 11281143]

[37]. Mahmood F, Hjorth Johannesen H, Geertsen P, Hansen RH. Diffusion MRI outlined viable tumour volume beats GTV in intra-treatment stratification of outcome. Radiother Oncol 2020;144:121–6.

[38]. Federau C, O'Brien K, Meuli R, Hagmann P, Maeder P. Measuring brain perfusion with intravoxel incoherent motion (IVIM): Initial clinical experience: Brain IVIM: Initial Clinical Experience. J. Magn. Reson. Imaging 2014;39(3):624–32. [PubMed: 24068649]

[39]. Zampini MA, Buizza G, Paganelli C, Fontana G, D'Ippolito E, Valvo F, Preda L, Baroni G. Perfusion and diffusion in meningioma tumors: a preliminary multiparametric analysis with Dynamic Susceptibility Contrast and IntraVoxel Incoherent Motion MRI. Magn Reson Imaging 2020;67:69–78. [PubMed: 31891760]

[40]. Sorensen AG, Batchelor TT, Zhang W-T, Chen P-J, Yeo P, Wang M, et al. A "Vascular Normalization Index" as potential mechanistic biomarker to predict survival after a single dose of cediranib in recurrent glioblastoma patients. Cancer Res 2009;69(13):5296–300. [PubMed: 19549889]

[41]. Kim C, Kim HS, Shim WH, Choi CG, Kim SJ, Kim JH. Recurrent glioblastoma: combination of high cerebral blood flow with MGMT promoter methylation is associated with benefit from low-dose temozolomide rechallenge at first recurrence. Radiology 2017;282(1):212–21. [PubMed: 27428890]

[42]. Harris RJ, Cloughesy TF, Hardy AJ, Liau LM, Pope WB, Nghiemphu PL, et al. MRI perfusion measurements calculated using advanced deconvolution techniques predict survival in recurrent glioblastoma treated with bevacizumab. J Neurooncol 2015;122(3):497–505. [PubMed: 25773062]

[43]. Meeus EM, Novak J, Dehghani H, Peet AC. Rapid measurement of intravoxel incoherent motion (IVIM) derived perfusion fraction for clinical magnetic resonance imaging. Magma. 2018;31:269–83. [PubMed: 29075909]

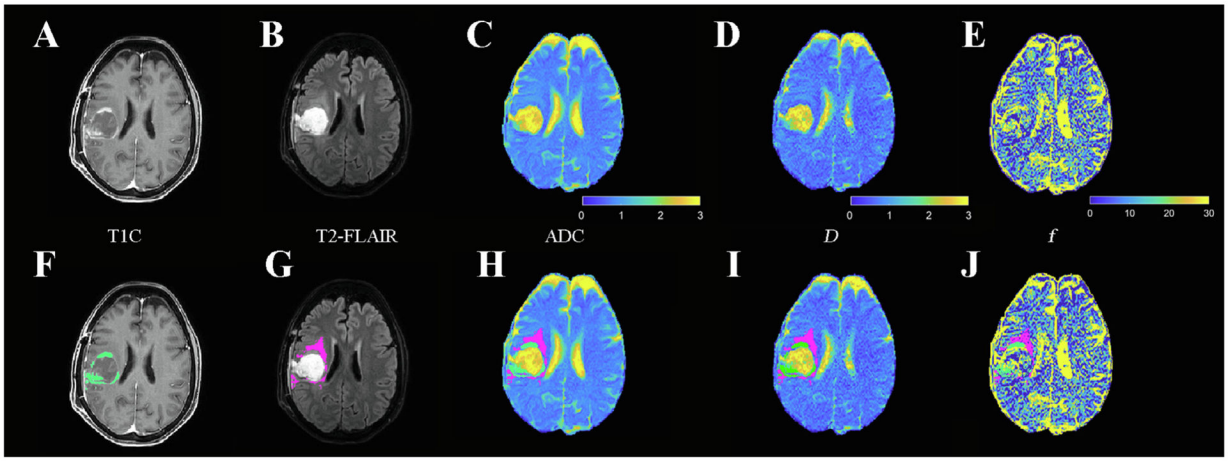

Fig. 1.

Images of a patient included in the study. Contrast-enhanced T1 image (A), T2-FLAIR image (B), ADC map (C), D map (D) and f map (E). Region of interest (green) of the enhancing parts of the mass (F), region of interest (magenta) of non-enhancing T2-FLAIR hyperintensity (G), with both regions of interest overlaid on ADC map (H), D map (I) and f map (J). ADC and D color bar scale is $\times 10^{-3}$ mm^2/s, while f color bar is shown in percent.

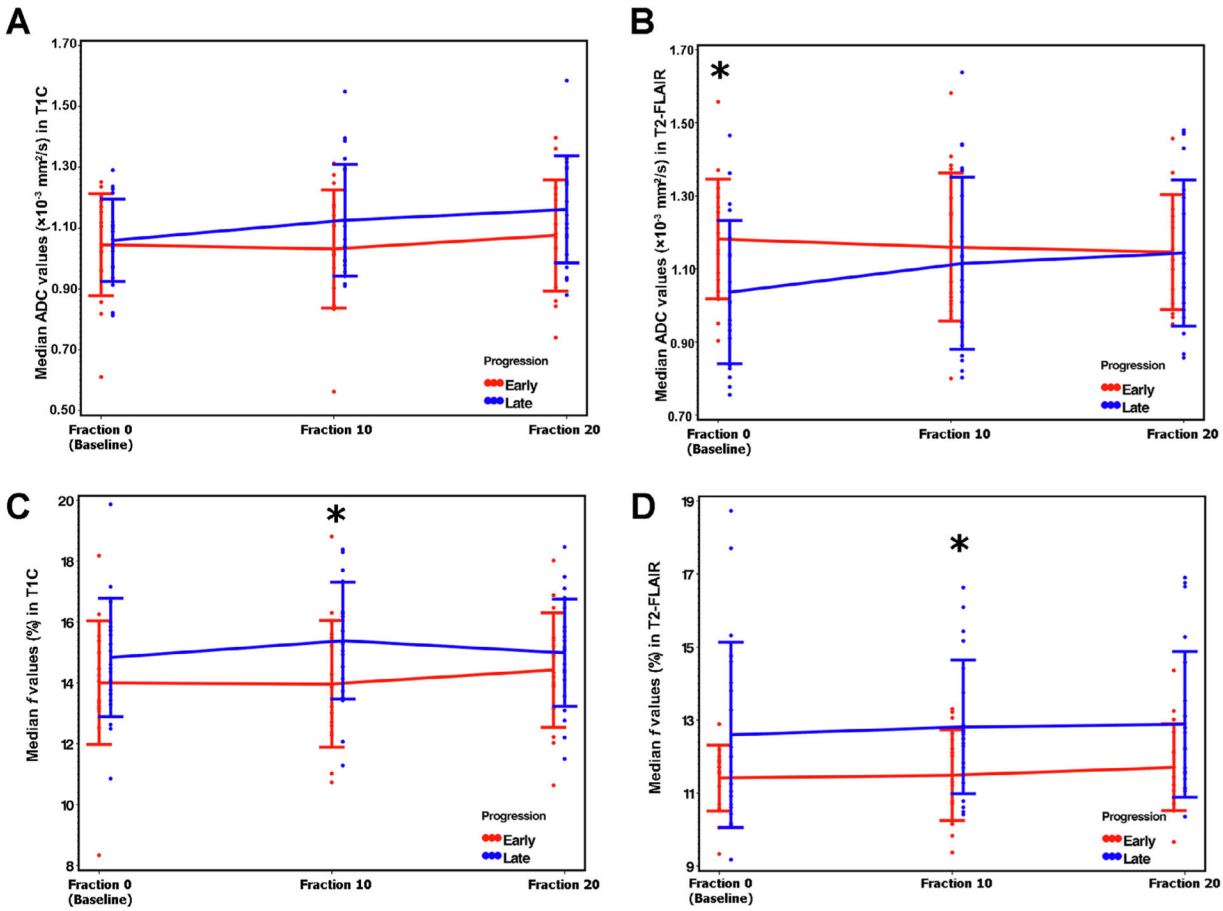

Fig. 2.

Changes in median ADC (A, B) and *f* (C, D) values during chemoradiation in T1 contrast-enhancing areas (A, C) and nonenhancing FLAIR hyperintense areas (B, D) stratified by early (red) vs. late (blue) progressors. Vertical lines represent one standard deviation, and stars (*) indicate where significant differences were observed.

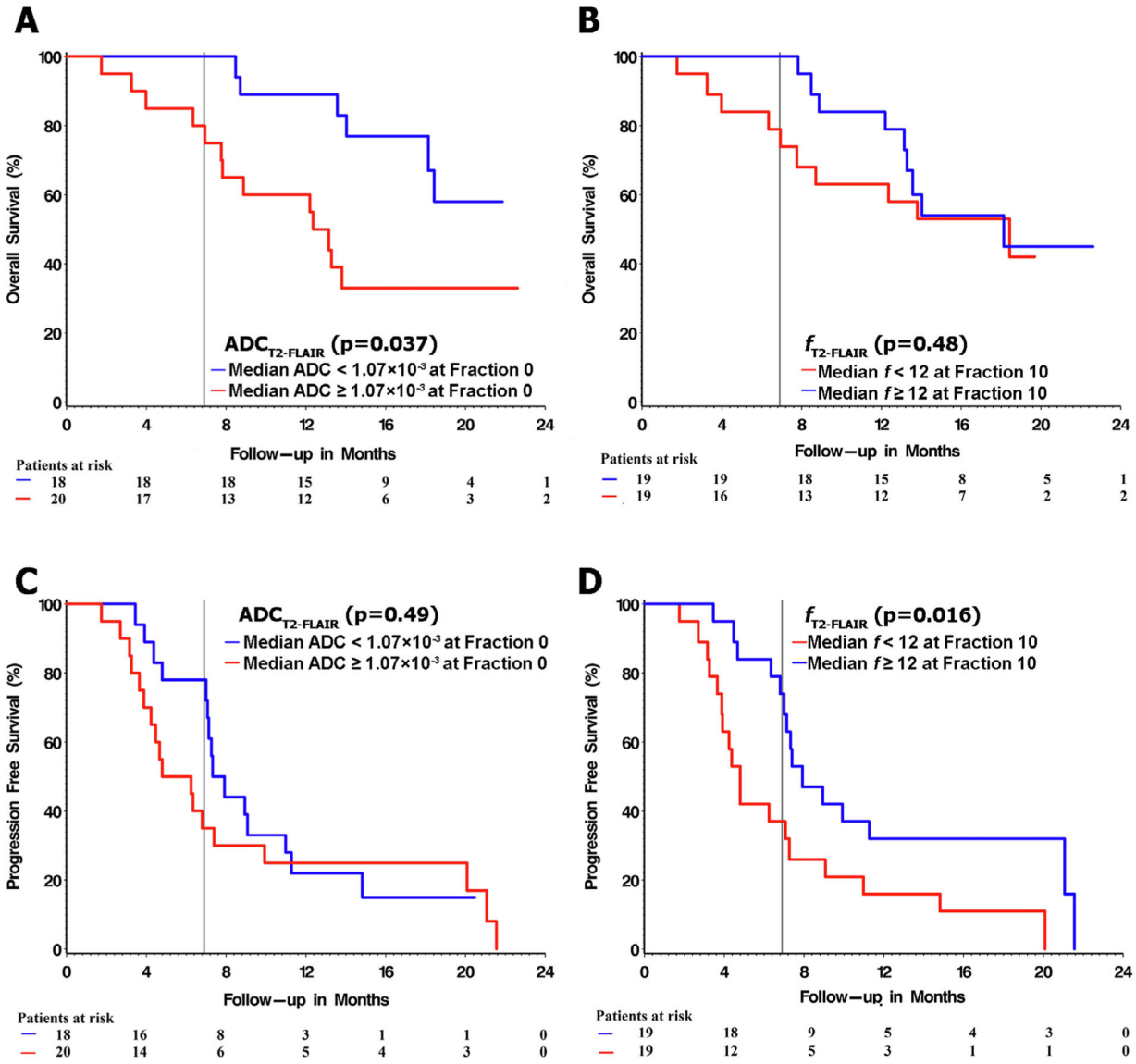

Fig. 3.

Kaplan-Meier analyses demonstrating the association with $ADC_{T2\text{-}FLAIR}$ (A, C) and $f_{T2\text{-}FLAIR}$ (B, D) on OS (A–B) and PFS (C–D). Grey vertical line on the plots indicates the 6.9 month timepoint which reflects the threshold for early vs. late progression used for this analyses.

Table 1

Patient demographics.

Patients	**All patients (*n* = 38)**	**Early progressors (*n* = 17)**	**Late Progressors (*n* = 21)***
Male (*n*, %)	25 (65.8%)	11 (64.7%)	14 (66.6%)
Median age at diagnosis (range)	57.50 (20–68)	57 (20–68)	58 (41–67)
MGMT promoter methylation			
Methylated	19 (50.0%)	7 (41.2%)	12 (57.1%)
Unmethylated	15 (39.5%)	9 (52.9%)	6 (28.6%)
Unknown	4 (10.5%)	1 (5.9%)	3 (14.3%)
ECOG at diagnosis			
0	24 (63.2%)	8 (47.1%)	16 (76.2%)
1	13 (34.2%)	8 (47.1%)	5 (23.8%)
2	1 (2.6%)	1 (5.9%)	0 (0%)
Extent of Resection			
Gross total resection (*n*, %)	9 (23.7%)	3 (17.6%)	6 (28.6%)
Sub-total resection (*n*, %)	22 (57.9%)	10 (58.9%)	12 (57.1%)
Biopsy Only (*n*, %)	7 (18.4%)	4 (23.5%)	3 (14.3%)
Median number of days between the baseline MRI and initiation of chemoradiation (range)	7 (0–14)	6 (0–14)	7 (7–12)
MRIs Completed			
Fraction 0 (*n*, %)	38 (100%)	17 (100%)	21 (100%)
Fraction 10 (*n*, %)	38 (100%)	17 (100%)	21 (100%)
Fraction 20 (*n*, %)	36 (94.7%)	16 (94.1%)	20 (95.2%)
Median time to progression (range) in months	7.2 (1.8–21.9)	4.3 (1.8–6.9) ***	11.1 (7.1–21.9) ***
Median follow-up (range) in months **	14.5 (1.8–27.9)	8.9 (1.8–18.2)	18.4 (8.6–27.9)

* At the date of last inquiry, 5 patients (13.2%) had not experienced progression of disease. As this date was > 6.9 months from baseline MRI, we considered these patients as late progressors.

** At the date of last inquiry, 18 patients (4 of the early progressors and 14 of the late progressors) were still alive and were therefore censored.

*** 2 patients progressed, one of whom passed away, prior to their standard of care 6–8 week post-treatment scan. Their date of death was used as their date of progression.

Table 2

Median and interquartile range (IQR) for ADC and *f*, stratified by outcome. Significant values as determined by univariate analysis are shown in bold, and show the association between the parameter with early progression.

		Baseline MRI		Fraction 10 MRI		Fraction 20 MRI	
Map	**Outcome**	**T1C**	**T2-FLAIR**	**T1C**	**T2-FLAIR**	**T1C**	**T2-FLAIR**
ADC (10^{-3} mm^2/s)	Early	1.05 (0.96–1.17)	**1.20 (1.07-1.27)**	1.02 (0.90–1.17)	1.11 (1.01–1.29)	1.08 (0.95–1.20)	1.14 (0.99–1.25)
	Late	1.06 (0.97–1.12)	**1.01 (0.91-1.14)**	1.06 (0.99–1.29)	1.07 (0.94–1.30)	1.14 (1.01–1.30)	1.11 (1.01–1.29)
	p-value	0.77	**0.029** *	0.14	0.53	0.16	0.97
f (%)	Early	14.1 (13.2–15.0)	11.7 (10.7–11.9)	**13.9 (12.6–15.5)**	**11.3 (10.7–12.5)**	14.3 (13.5–15.4)	11.6 (10.9–12.4)
	Late	14.6 (13.6–15.8)	12.0 (10.7–14.0)	**15.3 (14.1–16.4)**	**12.5 (11.7–13.8)**	15.1 (14.1–15.8)	12.2 (11.5–13.5)
	p-value	0.21	0.10	**0.045** *	**0.028** *	0.35	0.06

* After adjusting for ECOG and MGMT promoter methylation status, the significance for these variables were: $ADC_{T2\text{-}FLAIR}$, $p = 0.025$; $D_{T2\text{-}FLAIR}$, $p = 0.011$; f_{T1C}, $p = 0.018$; $f_{T2\text{-}FLAIR}$, $p = 0.039$.

Table 3

Cox regression analysis using median $ADC_{T2\text{-}FLAIR}$ from baseline, median $f_{T2\text{-}FLAIR}$ from fraction 10, adjusted for ECOG and MGMT promoter methylation status.

Outcome	Parameter	HR	95% CI	*p*-value
OS	Baseline median $ADC_{T2\text{-}FLAIR}$ (1.07×10^{-3} mm^2/s)	1.03	0.1–1.06	0.1
	Median $f_{T2\text{-}FLAIR}$ from fraction 10 (12%)	0.84	0.61–1.14	0.25
	ECOG 0 vs 1–2	**0.19**	**0.063–0.59**	**0.004**
	MGMT promoter methylation status (methylated vs unmethylated)	**0.28**	**0.096–0.8**	**0.017**
PFS	Baseline median $ADC_{T2\text{-}FLAIR}$ (1.07×10^{-3} mm^2/s)	1.01	0.99–1.04	0.43
	Median $f_{T2\text{-}FLAIR}$ from fraction 10 (12%)	**0.72**	**0.56–0.95**	**0.018**
	ECOG 0 vs 1–2	0.41	0.17–1.01	0.052
	MGMT promoter methylation status (methylated vs unmethylated)	**0.25**	**0.097–0.63**	**0.0033**

Significant values in **bold.**